

Indirect Measurement of Hepatic Drug Clearance by Fitting Dynamical Models

Yoko Franchetti*, Thomas D. Nolin[†] and Franz Franchetti[‡]

January 1, 2021

Abstract

We present an indirect signal processing-based measurement method for biological quantities in humans that cannot be directly measured. We develop the method by focusing on estimating hepatic enzyme and drug transporter activity through breath-biopsy samples clinically obtained via the erythromycin breath test (EBT): a small dose of radio-labeled drug is injected and the subsequent content of radio-labeled CO_2 is measured repeatedly in exhaled breath; the resulting time series is analyzed. To model EBT we developed a 14-variable non-linear reduced order dynamical model that describes the behavior of the drug and its metabolites in the human body well enough to capture all biological phenomena of interest. Based on this system of coupled non-linear ordinary differential equations (ODEs) we treat the measurement problem as inverse problem: we estimate the ODE parameters of individual patients from the measured EBT time series. These estimates then provide a measurement of the liver activity of interest. The parameters are hard to estimate as the ODEs are stiff and the problem needs to be regularized to ensure stable convergence. We develop a formal operator framework to capture and treat the specific non-linearities present, and perform perturbation analysis to establish properties of the estimation procedure and its solution. Development of the method required 150,000 CPU hours at a supercomputing center, and a single production run takes CPU 24 hours. We introduce and analyze the method in the context of future precision dosing of drugs for vulnerable patients (e.g., oncology, nephrology, or pediatrics) to eventually ensure efficacy and avoid toxicity.

1 Introduction

This paper introduces a signal processing based indirect measurement method for drug clearance activities of the liver in individuals, i.e., the elimination behavior of therapeutic drugs of interest. We provide the theoretical underpinning to estimate certain biological quantities that cannot be directly measured in live humans. An additional complexity we address arises from multiple biological processes that may dependently overlap and thus cannot be easily separated. Our work is set in the context of future personalized medicine and precision medicine applications, and thus focusses on establishing the necessary methodological and mathematical foundations for attempting such future applications.

More specifically, we present an indirect measurement method for enzyme and drug transporter activity in the liver of individual patients using a single probe, called *individualized physiologically based pharmacokinetic modeling of rate data (iPBPK-R)*. We set up a reduced order physiologically based pharmacokinetic (PBPK) model of the human body, i.e., a system of 14 coupled non-linear ordinary differential equations (ODEs) where drug concentration in tissues of interest are modeled as state variables. The model is accurate enough to capture all biological effects of interest while keeping the number of model parameters low for stable parameter estimation. We introduce a graph representation and an operator formalism to concisely capture and analyze the particular non-linearities involved, and to perform perturbation analysis to assess the quality of the estimation procedure.

*Department of Pharmaceutical Sciences, Center for Clinical Pharmaceutical Sciences, University of Pittsburgh School of Pharmacy, Pittsburgh, PA 15261 USA (e-mail: yof8@pitt.edu)

[†]Department of Pharmacy and Therapeutics, Center for Clinical Pharmaceutical Sciences, University of Pittsburgh School of Pharmacy, Pittsburgh, PA 15261 USA (e-mail: nolin@pitt.edu)

[‡]Department of Electrical and Computer Engineering, Carnegie Mellon University, Pittsburgh, PA 15213 USA

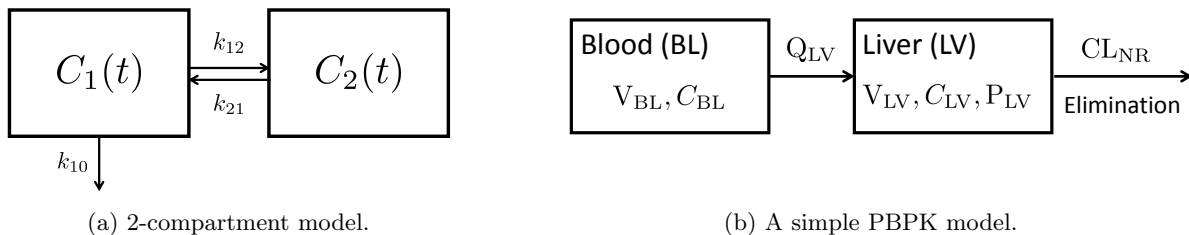


Figure 1: Compartmental pharmacokinetic models.

iPBPK-R solves an inverse problem to jointly estimate a set of ODE parameters that best fit a given measurement time series. These parameters provide indirect measurements for enzyme and transporter activity of interest. This is a hard optimization problem that needs to be carefully regularized via penalty terms and requires substantial computing resources, due the stiffness and non-linearity of the coupled ODEs and constraints imposed on the parameters by human biology. The method is implemented using R, and its development required 150,000 CPU hours on the *Bridges* supercomputer at Pittsburgh Supercomputing Center (PSC) [57].

For the development of the iPBPK-R method we leveraged data obtained in previous clinical research [34, 35], which was utilizing the erythromycin breath test (EBT): a small dose of the radio-labeled drug erythromycin is injected, and then the release rate of radio-labeled CO_2 in the patient’s breath is measured at eleven time points over two hours. This resolves the initial transient, the saturated maximum, and the terminal slope of drug behavior in the human body. Further, release *rate* of radioactive CO_2 carries higher information content than conventional concentration data. As an aside, the original EBT analysis procedure was simple and inconclusive, preventing clinical use of the EBT [26] [28]. We see potential future opportunities in utilizing a more advanced analysis method like iPBPK-R for not only EBT but other breath biomarker and probe development in this context since non-invasive breath biopsy research is emerging [7, 19].

Contribution. This paper introduces and analyzes the mathematical and computational engineering framework behind iPBPK-R, our method to *estimate* un-observable parameters related to drug clearance activity of the liver in *individuals*. The iPBPK-R method applies a classical signal processing approach in a biological setting. The purpose of this paper is to establish the mathematical and computational soundness of the method to enable future clinical research.

- We present both iPBPK-R’s general mathematical framework and the particular instance parameterized for the EBT as used in a previous clinical study [34, 35].
- iPBPK-R estimates biological quantities by solving a constrained optimization problem that fits a system of non-linear ODEs to clinical rate measurement data.
- We introduce a graph representation of the coupled system of non-linear ODEs and an operator formalism to model and linearize its state-dependent adjacency matrix.
- We utilize this formalism to provide a detailed mathematical analysis of the method, with focus on its constraints and the quality of its parameter estimates.

To provide context to the reader we summarize previously published applications of the method that estimate parameters related to drug clearance activity of the liver in individuals [14] [15]. Our method differs from the prevailing approach in the PBPK community since we do not predict drug behavior for a population, but *estimate* parameters for *individuals* given clinical measurement (breath) data. This paper is based on Chapter 2 of the dissertation thesis of Y Franchetti [13].

Synopsis. Sec. 2 provides the necessary background. Sec. 3–5 develop the underlying mathematical and pharmacokinetic approach. Sec. 6 shows clinical examples and applications while section 7 discusses the method and related work, followed by a conclusion in section 8.

2 Background

2.1 Mathematical Background

We briefly point to the mathematical concepts and methods used in this paper. The overall approach is following standard signal processing methodology [37]. We use graphs [?] and non-linear ODEs [24] to model the problem and non-linear operators [11, 12, 20, 21] to concisely describe the ODEs. We linearize these ODEs and use the theory of linear ODEs with constant coefficients to characterize the solutions via eigen decomposition of the system matrix [27]. We use perturbation analysis [25] to derive bounds and constraints.

We are estimating parameters of the ODEs to fit measurement data, as discussed in [33, 38, 41, 49, 50], and view the indirect measurement as inverse problem [4]. The approach leads to non-linear optimization problems [30, 31] that need to be regularized [1] and to be solved numerically [54, 61]. We implement the optimization in R [6].

2.2 Pharmaceutical Science Background

In the pharmaceutical industry PBPK modeling is typically used to predict drug concentration behavior over time. A system of ODEs is solved where each ODE is associated with a specific organ/tissue *compartment* and describes the flows of drug concentrations for that compartment [45]. In *population PBPK*, physiologically meaningful parameters are incorporated in the ODEs. Then, they are used to predict drug concentrations of the respective compartments for a population [32] [47] [23]. The prediction by PBPK modeling and simulation is informative for designing clinical trials and drug dosage.

However, all predictive models raise concerns regarding performance in *out-of-samples* settings where predictions are made outside of the data range, and thus have statistical uncertainty [18]. The physiological parameter inputs for these predictions are out-of-samples since equations to calculate the properties are typically developed based on multiple unrelated drug properties and thus extrapolate. The *in-vitro in-vivo extrapolation (IVIVE)* described later is one such common calculation technique [44] [40] [58].

In contrast, our approach performs *model fitting and parameter estimation*, not prediction. This change of viewpoint has a number of implications that we will discuss in section 7, chiefly that a smaller number of parameters is better to enable convergence to a unique solution, and that statistical considerations do not play a role. We now provide a quick overview of the relevant pharmaceutical science approaches.

Pharmacokinetics (PK). PK is the quantitative study of drugs and their metabolites over time in the body [46]. Compartmental models are developed with some parameters related to absorption, distribution, metabolism, and excretion (ADME) of drugs to describe the time dependency of drug concentration in the body. As example consider a two-compartment PK model for an intravenously dosed drug (see Fig. 1a), where the ODEs to describe the change in drug concentrations are given by

$$\dot{C}_1 = -(k_{10} + k_{12})C_1 + k_{21}C_2 \quad \text{and} \quad \dot{C}_2 = k_{12}C_1 - k_{21}C_2.$$

The concentration in Compartment 1 is given by

$$C_1(t) = Pe^{-\alpha t} + Qe^{-\beta t}$$

where the constants

$$P = \frac{A_0(\alpha - k_{21})}{V_1(\alpha - \beta)} \quad \text{and} \quad Q = \frac{A_0(k_{21} - \beta)}{V_1(\alpha - \beta)}$$

depend on A_0 , α , β , and V_1 that capture administered drug mass, distribution rate constant, disposition rate constant, and volume of distribution of Compartment 1, respectively. **Physiologically-based PK (PBPK).** PBPK modeling was developed in the 1930s [56] [45]. The entire body is viewed as a system and each organ/tissue is viewed as a compartment. A system of ODEs for the entire body is solved to evaluate the drug concentrations over time for each compartment. Physiological parameters are included so that the impact of particular physiological behavior on drug kinetics in the body can be evaluated. PBPK models require three components: (1) system-specific properties, (2) drug properties, and (3) the structure of the system adapted to the research problem [45].

See Fig. 1b for a simple PBPK model with blood (BL) and liver (LV) compartments and drug elimination from LV. The changes in drug concentration in BL and LV,

$$\begin{aligned}\dot{C}_{BL} &= Q_{LV} \left(\frac{C_{LV}}{P_{LV}} - C_{BL} \right) \quad \text{and} \\ \dot{C}_{LV} &= Q_{LV} (C_{BL} - \frac{C_{LV}}{P_{LV}}) - CL_{NR} C_{LV},\end{aligned}$$

form a system of ODEs where constants Q_{LV} , P_{LV} and CL_{NR} capture the blood flow into LV, the partition coefficient of LV to BL, and the drug clearance from LV, respectively.

IVIVE. IVIVE extrapolates the mean value of an *in vivo* (clinically relevant) physiological parameter as a function of a corresponding *in vitro* (experimentally/via bench work) obtained value [2] [44]. For example, metabolic clearance activity of CYP3A4 in human (*in vivo* clearance) for a particular drug can be calculated using [51] [5] as

$$CL_{H,int,3A4} = CL_{int,rh3A4} Abd_{3A4} ISEF_{3A4} MPPGL LW.$$

Here, $CL_{int,rh3A4}$ is the intrinsic clearance in recombinant CYP3A4 (*in vitro* clearance), Abd_{3A4} is the unit amount of CYP3A4 enzyme, $ISEF_{3A4}$ is intersystem extrapolation factor for CYP3A4, $MPPGL$ is the unit amount of microsomal protein, and LW is the human liver weight.

A value calculated via an IVIVE method is subject to substantial uncertainty. For example, experimentally determined $ISEF$ for CYP3A4 clearance has a large 95% confidence interval (CI) [40]. A calculated metabolic *in vivo* clearance may not have a strong correlation with experimentally determined *in vitro* metabolic clearance despite seemingly being linearly correlated in a log-log plot [5]. The relationship between IVIVE-predicted value and the observed *in vivo* value is a unique feature of a particular drug substrate. IVIVE-based generalization of such a relationship to other drugs produces a bias in predictions as this is an *out-of-samples* extrapolation.

Scaling factors are commonly derived from regression in a log-log plot, which does not predict *in vivo* metabolic clearance consistently. Therefore, it is not possible to estimate *a particular subject's* *in vivo* parameters using an IVIVE-derived scaling factor given the low predictive power and great uncertainty of this scaling factor. In contrast, we estimate an *adjustment factor* via PBPK modeling that measures an individual's deviation from the baseline IVIVE activity to *estimate* the individual's activity of a biological process.

2.3 Erythromycin Breath Test (EBT)

EBT was originally developed to measure CYP3A4 activity that metabolizes the radio-labeled drug ^{14}C -erythromycin in the liver [59]. EBT is based on the premise that as the drug undergoes the CYP3A4-mediated metabolic pathway, radio-labeled carbon dioxide ($^{14}CO_2$) is released as a final by-product. A subject receives a noninvasive, single intravenous (IV) bolus low dose of ^{14}C -erythromycin. Then, breath samples are collected at 11 time points within two hours of IV dosing, including the baseline time point (see Fig. 2b) [34] [35]. The sampling time points are unequally spaced. $^{14}CO_2$ production rates in the breath samples are calculated (as a percentage of dose exhaled per minute) at each time point from the exhaled volume and $^{14}CO_2$ content.

In the original EBT procedure breath samples are collected before and after a certain change in the subject's state. The resulting time series is used to detect *binary evidence (yes/no) of increase in CYP enzyme activity* as follows (see Fig. 2a): the CYP3A4 enzyme activity in the liver *increased if* (1) the time to peak of the breath rate shortened, *or* (2) the area under the curve increased, *or* (3) the measured $^{14}CO_2$ production rate at 20 minutes increased post the state change.

However, other physiological activities also seemed to affect elimination of the drug from the liver (e.g., activities in drug transporters) [17] [29] [16] [43] [42], and the original EBT criteria were inconclusively predicting CYP activity changes [26] [28]. iPBPk-R applied to EBT is revisiting the EBT analysis by taking advantage of $^{14}CO_2$ production rate data. Our approach suggests that more detailed modeling of EBT data can provide more granular information regarding CYP3A4 activity and other physiological factors.

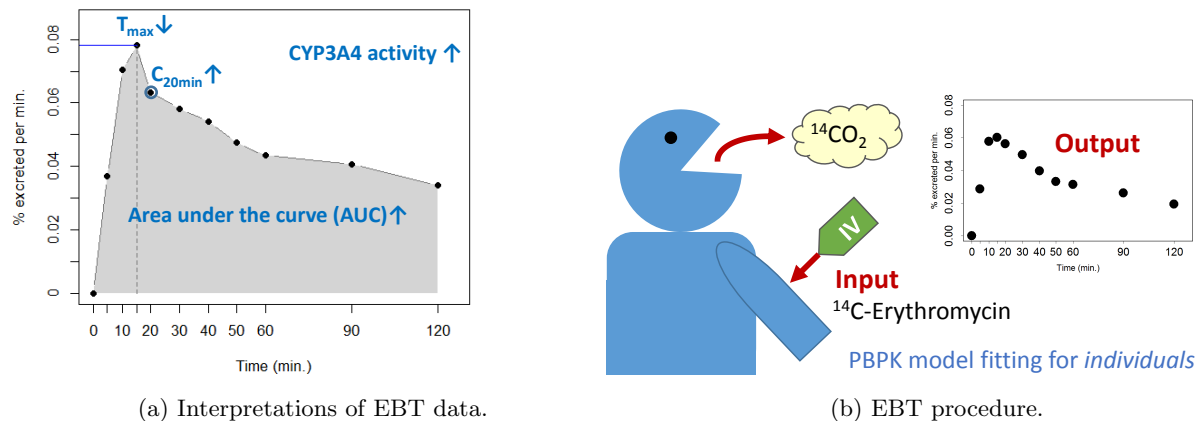


Figure 2: EBT and its classical interpretations.

3 Mathematical Framework of iPBPk-R

3.1 Overview

The key idea of iPBPk-R is to develop an *indirect measurement method* to simultaneously measure values in a particular patient for physiological parameters that cannot be measured directly. From an applied statistics perspective we are estimating parameters in a *within sampling* setting as opposed to *out-of-samples* setting; given clinically observed breath rate data from a single probe drug (i.e., EBT), PBPK model fitting (but not prediction) will be used to inversely solve for physiologically meaningful parameters explaining the response.

iPBPk-R is based on a reduced order PBPK model, which is parameterized by our physiological parameters of interest. Using measured breath rate data allows us to resolve the early transient (the impulse response) in the drug behavior at both rate-limiting and non-rate-limiting steps of multiple elimination pathways. IVIVE parameters are utilized as initial guesses that are adjusted for individual subjects based on their measurement data. Estimation is done via nested optimization or nested co-optimization and utilizes a specialized objective function (loss function). iPBPk-R enables us to estimate per-person physiological parameters which are otherwise difficult to capture, by utilizing observed concentration *change* data (production *rate* data), which at the same sampling rate and accuracy has higher information contents compared to drug *concentration* data. We develop the mathematical framework as follows. In section 3.2 we introduce a graph representation of the non-linear system of ODEs. Then in section 3.3 we introduce an operator formalism based on [11] [12] to capture the non-linearities in the model concisely, and in section 3.4 we formalize measurements and parameter estimation as optimization problem. This enables us to establish convergence properties in section 3.5 via perturbation analysis.

3.2 Reduced Model

In this subsection we describe the general shape of our reduced model. This model is underlying the modeling approach and is instantiated for EBT in section 4. Fig. 3 shows a simple three compartment model and all associated quantities used in the discussion below.

Compartments. The reduced model underlying iPBPk-R is given by a system of non-linear ordinary differential equations (ODEs) for time $t \geq 0$, described as a weighted directed graph (see Fig. 3)

$$G = (V, E, W) \quad \text{with} \quad E \subseteq V \times V. \quad (1)$$

The set of n vertices $V = \{V_1, \dots, V_n\}$ abstracts the compartments. Each compartment V_i has a state variable

$$m_i(t), \quad t \geq 0 \quad \text{with} \quad m_i(0) = M_i$$

that is a function of time and expresses the amount of drug mass in compartment V_i at time t .

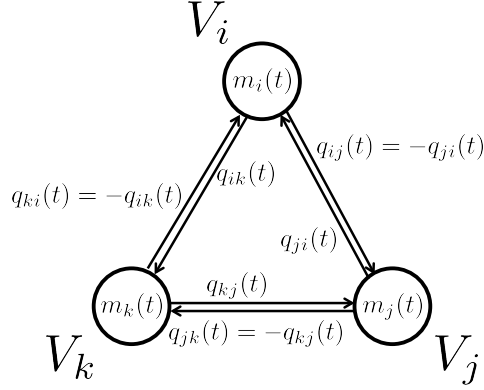


Figure 3: Example graph for a three compartment model.

Mass flows. Edges $e_{ij} = (V_i, V_j)$ and $e_{ji} = (V_j, V_i)$ in E together represent the channel between compartments V_i and V_j , viewed from the respective compartment. The weight $w_{ij} \in W$ on edge e_{ij} is given by the mass flow function

$$q_{ij}(t) = \dot{m}_i(t) \quad \text{for } e_{ij} \in E,$$

which expresses the flow of drug mass from compartment V_i into V_j over the edge e_{ij} as function of time t . We define $q_{kl}(t) \equiv 0$ if $e_{kl} \notin E$, i.e., for edges that do not exist. $q_{ij}(t)$ and $q_{ji}(t) = -q_{ij}(t)$ denote the same physical flow represented from the perspective of compartment V_i and V_j , respectively, as flow source. Thus the graph G has a $n \times n$ real-valued time-dependent anti-symmetric adjacency matrix

$$A(t) = [q_{ij}(t)]_{1 \leq i, j \leq n} \quad (2)$$

that concisely captures the system of non-linear ODEs of the reduced model.

State equations and invariants. Note that in our model some compartments V_i are *sources* for which all flows $q_{ij} \geq 0$ are non-negative (thus, they are out-flows), and some compartments V_i are *sinks* for which all flows $q_{ji} \geq 0$ are non-negative (thus, they are in-flows). The non-linearity of the model arises through non-linearities of certain flow terms $q_{ij}(t)$ that are induced through a Michaelis-Menten style saturation (see section 3.3).

For each compartment V_i the change of drug mass contents is the sum of all flows $q_{ji}(t)$ from all other compartments V_j into V_i , and there are no self-flows. Thus,

$$\dot{m}_i(t) = \sum_{j=1}^n q_{ji}(t) \quad \text{and} \quad \sum_{i=1}^n \dot{m}_i(t) = \sum_{i=1}^n M_i = M_0. \quad (3)$$

Since mass can only enter or leave a compartment V_i through a mass flow q_{ij} , the total mass in the system is constant M_0 .

Concentration based model. In Clinical Pharmacology it is common to express models via drug concentration and its time-dependent change

$$C_i(t) = \frac{m_i(t)}{V_i} \quad \text{and} \quad \dot{C}_i(t) = \frac{\dot{m}_i(t)}{V_i},$$

respectively (here V_i denotes the volume of the i th compartment), while mass-based equations allow for clearer mathematical treatment of the ODEs. Thus, in pharmacological discussions we will use $C(t)$ and $\dot{C}(t)$ while mathematical discussions will use $m(t)$ and $\dot{m}(t)$, respectively.

3.3 Reduced Model as Non-linear ODE System

We now define a framework that allows us to describe the system of non-linear ODEs (3) via the time-dependent adjacency matrix (2) similar to how a system of linear first order ODEs with constant coefficients is described through its constant system matrix.

Definitions and conventions. When needed to disambiguate vectors and scalars, vectors $x \in \mathbb{R}^n$ are annotated as \vec{x} . Entries of the vector x are denoted as x_i , and the vector x can be written as $x = (x_i)_{1 \leq i \leq n}$. Real $m \times n$ matrices are denoted as $\mathbf{A} = [a_{ij}]_{1 \leq i \leq m, 1 \leq j \leq n}$.

The *Michaelis-Menten* function $\text{MM}_{a,b,c}$ is a homogeneous hyperbolic function that is parameterized by three constants a, b , and c ,

$$\text{MM}_{a,b,c}(x) = \frac{ax}{b + cx}. \quad (4)$$

It is the main non-linearity used in the reduced model, and it is a monotonically increasing differentiable function. The parameters capture the initial slope and the asymptotic value of the function. We denote a function $f(\cdot)$ that depends on a parameter vector p as $f^p(\cdot)$. In our case the parameters p_i that constitute the vector p are to be optimized during estimation.

Notation for non-linear operators. We unify the notation for linear and non-linear operators $\mathbf{A}(\cdot)$ that map vectors to vectors. This will allow us to analyze and linearize the non-linear system of ODEs (3), and to obtain a good characterization of the original non-linear system with respect to parameter estimation. A matrix $\mathbf{A} \in \mathbb{R}^{m \times n}$ defines a linear operator

$$\mathbf{A}(\cdot) : \mathbb{R}^n \rightarrow \mathbb{R}^m; x \mapsto \mathbf{A}(x) = \mathbf{A}x,$$

and we use the notation $\mathbf{A}(\cdot)$ for a matrix \mathbf{A} to denote its interpretation as operator.

We next generalize the matrix-vector product to matrices where the entries are scalar functions. Assume that entries at location (i, j) of a $m \times n$ matrix \mathbf{B} are scalar functions

$$b_{ij}(\cdot) : \mathbb{R} \rightarrow \mathbb{R}; x \mapsto b_{ij}(x). \quad (5)$$

We use \mathbf{B} to define the *non-linear operator* $\mathbf{B}(\cdot)$ as

$$\mathbf{B}(\cdot) : \mathbb{R}^n \rightarrow \mathbb{R}^m; \mathbf{B}(x) = y \quad \text{with} \quad y_i = \sum_{j=1}^n b_{ij}(x_j). \quad (6)$$

The definition of $\mathbf{B}(\cdot)$ generalizes the standard matrix-vector product. Finally, we define operator addition $\mathbf{U}(\cdot) + \mathbf{V}(\cdot)$ as

$$(\mathbf{U}(\cdot) + \mathbf{V}(\cdot))(x) = \mathbf{U}(x) + \mathbf{V}(x), \quad (7)$$

compatible with the usual addition of matrices.

Reduced model ODE as non-linear operator. We now describe the non-linear system of ODEs concisely as a sum of operators. Our state vector is the vector of mass in all compartments of the n -compartment model, $\vec{m} = (m_i)_{1 \leq i \leq n}$. The forcing function $z(t)$ is zero everywhere except for the k th component $z_k(t) = \tau$ in the interval $[0, t_0]$ to model intravenous (IV) injection into the vein compartment.

The linear part of the system of ODEs is given by a real $n \times n$ matrix \mathbf{X} . All non-linearities are collected in the $n \times n$ matrix of scalar functions $\mathbf{Y} = [y_{ij}(\cdot)]_{i,j}$ where all entries $y_{ij}(\cdot)$ are either the *zero function* $o(x) \equiv 0$, a single Michaelis-Menten function (4), or a sum of two Michaelis-Menten functions (4). The matrix of functions \mathbf{Y} is used to describe the operator $\mathbf{Y}(\cdot)$ as defined in (6). With these definitions, the full non-linear system of ODEs is given by

$$\dot{m} = \mathbf{M}(m) + z(t) \quad \text{with} \quad \mathbf{M}(\cdot) = \mathbf{X}(\cdot) + \mathbf{Y}(\cdot). \quad (8)$$

$\mathbf{M}(\cdot)$ is the state-dependent adjacency matrix (2). Analysis of the solution of (8) and convergence and uniqueness of parameter estimation via optimization is reduced to analyzing \mathbf{M} . In addition, the non-linear behavior of \mathbf{M} is limited to Michaelis-Menten saturation. This enables us to analyze solution properties of (8) via perturbation analysis of the entries of \mathbf{M} , and by analyzing the linearized bounds of \mathbf{M} .

3.4 Measurements and Parameter Estimation

Measurement. Next we model the pathway of the drug by-product $^{14}\text{CO}_2$ from the liver to the breath and its ultimate concentration measurement in the breath. This is described as a measurement operator $\mathcal{F}(\cdot)$ that maps the solution vector $\vec{C}(t)$ of (8) (in drug concentration form) to a scalar function $B(t)$. Under the

assumption of instant metabolism of the drug in the liver and instant transfer of $^{14}\text{CO}_2$ from liver to lung, the operator $\mathcal{F}(\cdot)$ just returns the first derivative of the liver compartment (denoted as j th compartment), i.e.,

$$B(t) = \mathcal{F}(\vec{C}(t)) = \dot{C}_j(t). \quad (9)$$

More realistic variants of $\mathcal{F}(\cdot)$ can be defined to model the transfer of $^{14}\text{CO}_2$ from the liver to the lung more accurately, and we provide further details in section 5.

Comparing model and measurement. Next we define a distance function from $B(t)$ as defined in (9) to clinical breath rate measurements. A measurement consist of T samples $m_\ell = (t_\ell, w_\ell)$ measuring $^{14}\text{CO}_2$ production rate taken at time points t_ℓ , arranged as a vector of 2D points, $\vec{S} = ((t_\ell, w_\ell))_\ell$ for $\ell = 1, \dots, T$. We define a *distance function* $d(\cdot, \cdot)$ to denote the distance (or disagreement) between the simulated function and the sampled data. A straight-forward example for a distance function $d(\cdot, \cdot)$ is the L_2 norm of the breath function $B(t)$ evaluated at the sample time points t_ℓ minus the measured data at the same time points,

$$d_2(B(\cdot), \vec{S}) = \|(B(t_\ell))_\ell - (w_\ell)_\ell\|_2, \quad \ell = 1, \dots, T, \quad (10)$$

which is provided to aid the discussion regarding parameter estimation. We present the more complex definition and detailed discussion of the actually used distance functions in section 5.

Parameter estimation via optimization. The estimation of biological parameters is cast as an optimization problem that fits a dynamical model (system of ODEs) to measurement data. The biological parameters of interest are derived from the estimated ODE parameters that produce the best fit. We aim to find a vector \vec{r} that parameterizes the system of ODEs (8) (in concentration form) so that the distance $d(\cdot, \cdot)$ from a given measurement vector \vec{S} is minimized. Further, constant parameters are captured by a parameter vector \vec{u} . Therefore the flow terms $q_{ij}(t)$ in (3) and the solution of this system of ODEs $\vec{C}(t)$ are parameterized by \vec{r} and \vec{u} and need to be written as

$$q_{ij}^{\vec{r}, \vec{u}}(t) \quad \text{and} \quad \vec{C}^{\vec{r}, \vec{u}}(t),$$

respectively. The parameter estimation is set up as the optimization problem

$$\vec{r} = \arg \min_{\vec{r}'} \Psi^{\vec{u}}(\vec{r}') \quad \text{for configuration } \vec{u} \quad (11)$$

for a specialized objective function

$$\Psi^{\vec{u}}(\vec{r}) = d(\mathcal{F}(\vec{C}^{\vec{r}, \vec{u}}(\cdot)), \vec{S}) + \pi(\vec{r}, \vec{u}) \quad (12)$$

with appropriately chosen distance $d(\cdot, \cdot)$ and penalty term $\pi(\vec{r}, \vec{u})$. To ensure the that the estimation returns biologically plausible values and adjustment factors are as close to 1 as possible, the penalty function $\pi(\cdot, \cdot)$ needs to be chosen carefully. The penalty term is defined as

$$\pi(\vec{r}, \vec{u}) = u_b \nu(\vec{r}) + u_c \rho(\vec{r}) + u_d \epsilon(\vec{r}) + u_x \psi(\vec{r}). \quad (13)$$

The terms $\nu(\vec{r})$, $\rho(\vec{r})$, $\epsilon(\vec{r})$, and $\psi(\vec{r})$ are constraint or penalty terms that depend on the parameter vector \vec{r} , and the constants u_b , u_c , u_d , and u_x are weighting factors that are collected in the configuration vector \vec{u} . The exact forms of the penalty terms will be discussed in section 5.

3.5 Analysis of iPBPk-R Estimation

In this section we establish that parameter estimation (as it is set up in section 3.4) is converging as long as good starting values (in our case IVIVE estimates) are known and the number of estimated parameters is properly bounded.

Linearization of the system of ODEs. The nonlinear ODE system eq. (8) can be bounded as

$$(\mathbf{X} + \mathbf{Y}^-)\vec{m}(t) + \vec{z}(t) \preceq \frac{d\vec{m}(t)}{dt} \preceq (\mathbf{X} + \mathbf{Y}^+)\vec{m}(t) + \vec{z}(t)$$

(\preceq denotes *element-wise* comparison) where

$$\begin{aligned} \mathbf{Y}^- &= [y_{ij}^-]_{i,j=1,\dots,n} \quad \text{with} \quad y_{ij}^- = \min_{t \geq 0} \dot{y}_{ij}(m_j(t)) \quad \text{and} \\ \mathbf{Y}^+ &= [y_{ij}^+]_{i,j=1,\dots,n} \quad \text{with} \quad y_{ij}^+ = \max_{t \geq 0} \dot{y}_{ij}(m_j(t)). \end{aligned}$$

\mathbf{Y}^- and \mathbf{Y}^+ are matrices representing elementwise upper and lower bounds on the matrix elements of \mathbf{Y} . Therefore,

$$y_{ij}^- m_j(t) \leq y_{ij}(m_j(t)) \leq y_{ij}^+ m_j(t) \quad (14)$$

holds for all matrix elements of \mathbf{Y} for all $t \geq 0$. For iPBPK-R to produce stable parameter estimates, the distance between the boundaries $|y_{ij}^+ - y_{ij}^-|$ needs to be small enough. Then arguments for the linearized upper and lower bounds hold for the non-linear system of ODEs. The exact bounds are problem dependent and can be checked post-hoc.

Solution of linearized ODE. The solution $\vec{x}(t)$ of a homogeneous system of n linear ODEs with a *simple* real system matrix \mathbf{A} (which has n linearly independent eigenvectors),

$$\frac{d\vec{x}(t)}{dt} = \mathbf{A}\vec{x}(t), \quad \vec{x}(t) \in \mathbb{R}^n, \quad \mathbf{A} \in \mathbb{R}^{n \times n}, \quad t \geq 0 \quad (15)$$

is given by

$$\vec{x}(t) = \sum_{i=1}^n \beta_i \vec{c}_i e^{\theta_i t} \quad \text{with} \quad \vec{x}(t) = (x_j(t))_{j=1,\dots,n}. \quad (16)$$

We denote eigenvalues and eigenvectors of the system matrix \mathbf{A} as θ_i and \vec{c}_i , respectively, and the only eigenvalue with multiplicity greater than 1 is $\theta_0 = 0$. In our application $\mathbf{A}^- = (\mathbf{X} + \mathbf{Y}^-)$ and $\mathbf{A}^+ = (\mathbf{X} + \mathbf{Y}^+)$, and we ignore the forcing function $\vec{z}(t)$ since $\vec{z}(t) \equiv 0$ for $t > t_0$. The j th element of $\vec{x}(t)$ is the scalar solution for the j th compartment,

$$x_j(t) = \sum_{i=1}^n \beta_i c_{j,i} e^{\theta_i t} \quad \text{where} \quad \vec{c}_i = (c_{j,i})_{j=1,\dots,n}.$$

The function $x_j(t)$ is the projection of $\vec{x}(t)$ into the j th dimension (i.e., j th compartment).

Construction of ODE solution from projection. We now derive the conditions under which *the entire solution* $\vec{x}(t)$ of eq. (15) can be reconstructed from the j th dimension. A measurement consists of T samples $(t_\ell, x_j(t_\ell))_\ell$ of the function $x_j(t)$. Under our assumptions the (normalized) eigenvectors \vec{c}_i are functions of the eigenvalues θ_i . This allows us to set up a non-linear system of $2n$ equations in β_i and θ_i ,

$$x_j(t_\ell) = \sum_{i=1}^n \beta_i c_{j,i}(\theta_i) e^{\theta_i t_\ell} \quad \text{for} \quad \ell = 1, \dots, T. \quad (17)$$

Thus, at least $2n$ observed samples are necessary to estimate the $2n$ unknown values β_i and θ_i . More samples lead to better estimates via solving a non-linear least squares problem. Higher multiplicity of $\theta_0 = 0$ does not pose a problem as the nullspace of \mathbf{A} captures the source and sink of the dynamical system for which we do not need unique solutions.

Perturbation of ODE for the linearized system. We define a small perturbation $\alpha = (1 + \varepsilon) \approx 1$ for a matrix entry a_{ij} , i.e., replace a_{ij} with αa_{ij} and view the resulting matrix $\tilde{\mathbf{A}}$ as a function of α , i.e., $\tilde{\mathbf{A}}(\alpha)$. For small enough α the eigenvalues of $\tilde{\mathbf{A}}$ depend continuously and differentiably on α . This can be shown by using Laplace's formula for the determinant, Cramer's solution formula for linear systems, and the fundamental theorem of algebra. Thus, for a small enough α the partial derivatives

$$\frac{\partial \theta_i}{\partial \alpha} \quad \text{and} \quad \frac{\partial \beta_i}{\partial \alpha}$$

exist at least locally under weak assumptions that are met in practice by iPBPK-R. The above discussion generalizes to multiple perturbations α_i .

Parameter estimation for the linearized system. The set of T non-linear equations (17) can be recast as non-linear least squares problem for $\vec{\alpha} = (\alpha_1, \dots, \alpha_M)$,

$$\vec{\alpha} = \arg \min_{\vec{\alpha} \in \mathbb{R}^M} \sum_{\ell=1}^T \left(x_j(t_\ell) - \sum_{i=1}^n \beta_i(\vec{\alpha}) c_{j,i}(\vec{\alpha}) e^{\theta_i(\vec{\alpha}) t_\ell} \right)^2$$

that has at least one solution that can be found for initial values close to the optimum. Thus, the adjusted system matrix $\tilde{\mathbf{A}}(\vec{\alpha})$ needs to be close to the matrix \mathbf{A} , which is derived from IVIVE parameters. The local minimum $\vec{\alpha}$ closest to $\mathbf{1}_M = (1, \dots, 1)$ is the most *biologically plausible* estimate. Since θ_i are the roots of the characteristic polynomial of eq. (15) of degree n , at maximum n independent perturbations α_i can be estimated, and at least $2n$ data points $x_j(t_\ell)$ are needed.

Parameter estimation for nonlinearity. Recall that all non-linearities are of Michaelis-Menten form and have two true parameters (initial slope at 0 and maximum value at infinity). The nonlinear Michaelis-Menten saturation suppresses the peaks of the exponential terms in the solution $\vec{x}(t)$ and thus the shapes of the solution-time curves deviate from those of the corresponding pure exponential terms, in particular for high values of $\|\vec{x}(t)\|$. This happens in the initial transient of the solution. To estimate such nonlinearities, observed samples around the peaks of the exponentials are required. At least 2 samples per nonlinear Michaelis-Menten term in a adjustment factor α_i are needed to estimate its two parameters.

Summary. Our analysis shows that the iPBPk-R approach allows us under the following practical conditions to obtain reasonably accurate parameter estimates via optimization:

- 1) The distance $|y_{ij}^+ - y_{ij}^-|$, needs to be small enough to produce stable parameter estimates.
- 2) At maximum n *functionally independent* adjustment factors α_i in the linearized matrix can be estimated.
- 3) At maximum n nonlinearities (2 parameters per nonlinear term) can be estimated.
- 4) A solution is guaranteed and can be investigated to assess its stability and plausibility.
- 5) Since iPBPk-R solves a nonlinear high-dimensional optimization problem, there is no guarantees that the global optimum is found.
- 6) The objective function $\Psi^{\vec{r}, \vec{a}}(\cdot)$ introduces penalty terms to push the optimization towards the biologically most plausible parameter solution.
- 7) Good starting values (e.g., values chosen based on IVIVE for biological plausibility) are absolutely essential. The discussion in this section provides a worst-case estimate and bounds. In particular, a smaller number of modes θ_i may be relevant and observable in the measurement compartment j , and all scaling factors α_i may be acting only on these modes.

4 The PBPK Model underlying iPBPk-R for EBT

In this section we provide the detailed model description of iPBPk-R as used for the EBT as an instance of the framework laid out in section 3. We provide the classical view of the PBPK compartment model in section 4.1 and then translate it into our framework for analysis in section 4.2. For readability we are collecting all parameters and detailed formulas in table 3–table 5 in the appendix.

4.1 Developing the Reduced Model

Model setup. The core of our system is a seven-compartmental PBPK model of ^{14}C -erythromycin as shown Fig. 4, depicting the ODE system of ^{14}C -erythromycin. The model contains compartments for artery, vein, lung, kidney, extracellular space, liver cells, and combined other organs. Further, there are supporting source and sink compartments used for mass balance that capture IV dosing, exponential decay in other organs, urine, bile, and metabolic by-product $^{14}\text{CO}_2$. Our ODE system is a minimum full model according to Sager et al. [48] but can be also viewed as a reduced order model since the number of compartments are limited so that parameters in the model are estimable. Building an iPBPk-R model (in our case of $^{14}\text{CO}_2$ production rate in healthy subjects) entails defining compartments (Fig. 4 and Fig. 5) and flow terms between the compartments (table 3–table 4).

Mass flows. The mass flows $q_{ji}(t)$ in eq. (3) are expressed as a function of drug concentration C_i and C_j in the compartments V_i and compartment V_j , respectively, and parameterized by a vector of adjustment factors,

$$\vec{r} = (\alpha_k, \beta_k, \gamma_k, \gamma_i, \gamma_j, \lambda_k, \kappa_{ij}) \quad (18)$$

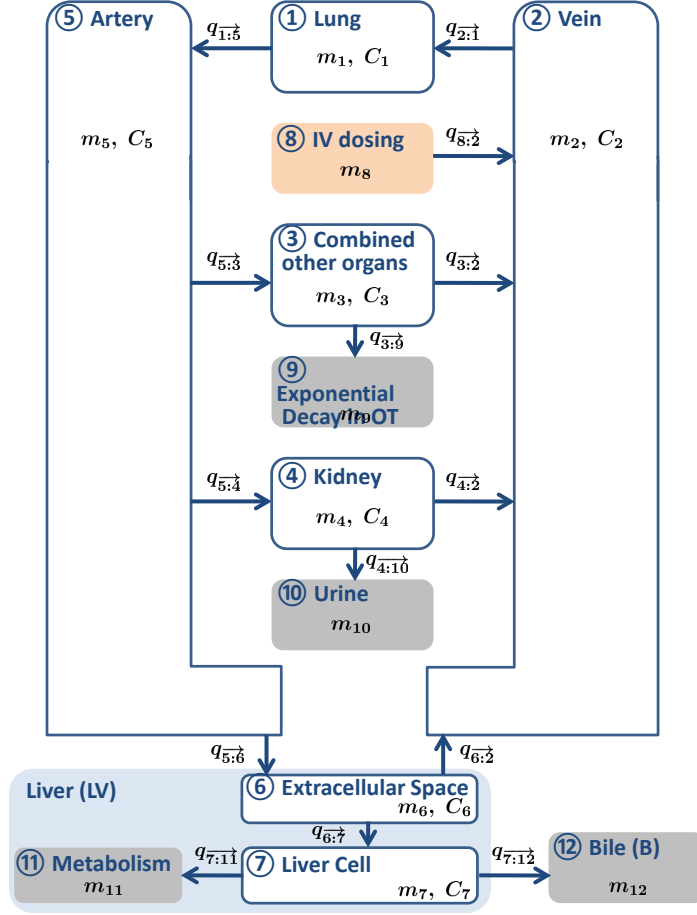


Figure 4: The ODE system of ^{14}C -erythromycin in iPBPK-R. Adapted from Franchetti et al. [14] with permission of American Society for Pharmacology and Experimental Therapeutics (ASPET).

(see table 4), which will be optimized for parameter estimation (see section 5).

Mass flows are captured by three types \mathcal{Q}_1 , \mathcal{Q}_2 , or \mathcal{Q}_3 shown in (20)–(22) below. A flow term $q_{ji}(t)$ is given by a single such term or a combination of two or three terms of the mass flows types,

$$q_{ji}^{\vec{r}, \vec{u}}(t) = \begin{cases} (-1)^{\delta_{ki}} \mathcal{Q}_1^{\vec{r}_1} \text{ or } (-1)^{\delta_{ki}} \mathcal{Q}_2^{\vec{r}_2} \text{ or } \mathcal{Q}_3^{\vec{r}_3} \\ (-1)^{\delta_{ki}} (\mathcal{Q}_1^{\vec{r}_1} + \mathcal{Q}_2^{\vec{r}_2}) \\ (-1)^{\delta_{ki}} (\mathcal{Q}_1^{\vec{r}_1} + \mathcal{Q}_2^{\vec{r}_2}) + \mathcal{Q}_3^{\vec{r}_3}. \end{cases} \quad (19)$$

Here, $\vec{r}_1 = (\alpha_k, \gamma_k)$, $\vec{r}_2 = (\alpha_k, \gamma_k, \beta_k, \lambda_k, h)$, and $\vec{r}_3 = (\kappa_{ij}, \gamma_i, \gamma_j)$, \vec{u} is a configuration vector, $h, k \in \vec{u}$ are configuration constants, where $h = 0/1$ implies competitive/non-competitive mass flow inhibition and $k = i$ or j . δ_{mn} is the Kronecker delta function (0 for $m \neq n$ and 1 otherwise).

\mathcal{Q}_1 is linearly proportional to the drug concentration C_k of a single compartment,

$$\mathcal{Q}_1^{(\alpha_k, \gamma_k)} = \alpha_k K_{k,1} \frac{L_k}{\gamma_k P_k} C_k, \quad k = i \text{ or } j, \quad (20)$$

with IVIVE constants $K_{k,1}$ (clearance) and L_k (captures fraction unbound). \mathcal{Q}_2 is nonlinearly proportional to the drug concentration C_k of a single compartment,

$$\mathcal{Q}_2^{(\alpha_k, \gamma_k, \beta_k, \lambda_k, h)} = \frac{\beta_k^{\delta_{0h}} K_{k,21} \frac{L_k}{\gamma_k P_k} C_k}{\lambda_k^{\delta_{1h}} K_{k,22} + \frac{L_k}{\gamma_k P_k} C_k}, \quad k = i \text{ or } j, \quad (21)$$

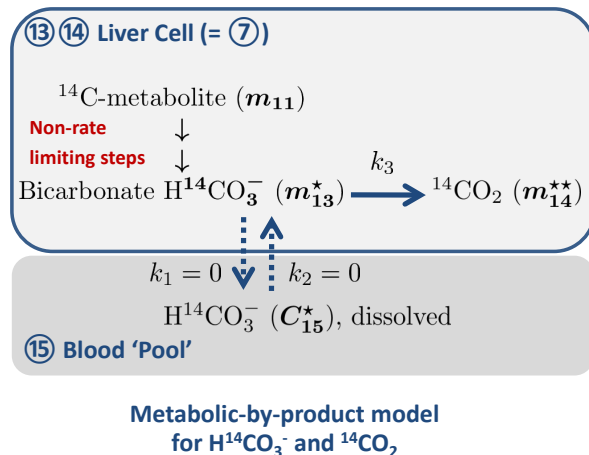


Figure 5: The metabolic by-product model in iPBPK-R.

with IVIVE constants $K_{k,21}$ (maximum drug mass flow), and $K_{k,22}$ (drug concentration where 50% of $K_{k,21}$ is achieved). Q_3 is proportional to the difference in drug concentration between compartments C_i and C_j ,

$$Q_3^{(\kappa_{ij}, \gamma_i, \gamma_j)} = \kappa_{ij} \left(K_{j,3} \frac{L_j}{\gamma_j P_j} C_j - K_{i,3} \frac{L_i}{\gamma_i P_i} C_i \right), \quad (22)$$

where $K_{i,3}$ and $K_{j,3}$ combine multiple IVIVE values.

Vein and artery compartments. In iPBPK-R, Vein and Artery compartments were separately modeled. This differs from classical PBPK models where in clinical pharmacology blood tissue is viewed as one compartment. In the connection from Artery, Extracellular Space, through to Vein compartment, we assumed the two algebraic relationships (see Fig. 4). First, the mass flow from Artery to Extracellular Space $q_{5,6}$ is fast and thus modeled instantaneous as $C_{5|6} = C_6$. Second, we assumed the 2-blood compartment model (i.e., a model with Vein and Artery compartments) for the blood tissue to be well-stirred, which necessitated a second algebraic relationship

$$C_{2|6} = \frac{C_6}{P_6}.$$

Both are necessary assumptions in iPBPK-R to approximate the drug flows between the blood tissue and liver organ when the blood is modeled with two separate compartments, Artery and Vein, while retaining the well-stirred model assumption for the blood tissue.

Modeling $^{14}\text{CO}_2$ dynamics. Beyond the drug and its metabolite, $^{14}\text{CO}_2$ production rate in the EBT needs to be modeled, which we conduct via a one-compartment metabolic-by-product model following [55] (Fig. 5). Given the separation of time scales between the drug dynamics and the $^{14}\text{CO}_2$ dynamics, we model ^{14}C -erythromycin as converted to its metabolite and by-product $\text{H}^{14}\text{CO}_3^-$ in the CYP3A4-mediated pathway instantaneously and the subsequent final-by-product $^{14}\text{CO}_2$ transported instantaneously to the lung and exhaled. This implies the two rate constants k_1 and k_2 from [55] are set to 0, which is supported by an in vivo rat study. Thus, $^{14}\text{CO}_2$ gets released from $\text{H}^{14}\text{CO}_3^-$ in the liver cell with an excretion rate constant k_3 and is instantaneously measured in the breath. C_{13}^* and C_{15}^* denotes the concentration of $\text{H}^{14}\text{CO}_3^-$ in the liver cell and in the blood pool. The respired amount of $\text{H}^{14}\text{CO}_3^-$ and exhaled $^{14}\text{CO}_2$ have a one-to-one molar relationship. The amount of $^{14}\text{CO}_2$ in the breath is denoted by m_{14}^{**} (see [14]).

4.2 Matrix Representation of the PBPK Model

In this section we present the reduced model used in iPBPK-R in the formalism described in section 3.3. The full non-linear system of ODEs is written as

$$\frac{d\vec{m}(t)}{dt} = \mathbf{X}\vec{m}(t) + \tilde{\mathbf{Y}}(\mathbf{D}\vec{m}(t)) + z(t). \quad (23)$$

Non-zero entries $x_{i,j}$ of \mathbf{X} , $y_{i,j}(\cdot)$ of $\tilde{\mathbf{Y}}$, and d_i of the diagonal matrix \mathbf{D} are provided in table 5. The diagonal elements d_i pre-scale the vector elements $m_i(t)$ before $\tilde{\mathbf{Y}}(\cdot)$ is applied and can be propagated into the parameters of the $y_{i,j}(\cdot)$ using the identity

$$\text{MM}_{a,b,c}(\alpha x) = \text{MM}_{\alpha a,b,\alpha c}(x).$$

This allows us to convert (23) into the normal form given by (8) with system operator matrix

$$\mathbf{A}(\cdot) = \mathbf{X}(\cdot) + \mathbf{Y}(\cdot) \quad \text{with} \quad \mathbf{Y}(\cdot) = \tilde{\mathbf{Y}}(\cdot) \circ \mathbf{D}(\cdot).$$

The forcing function $z(t)$ follows the shape discussed in section 3. It models injecting the drug at a dosing rate $\tau = M_0/t_0$ for the short dosing interval $\Omega = [0, t_0]$ into the Vein compartment. In (23) and table 5 we omit the bicarbonate concentration in the pool compartment, C_{15}^* , since $k_1 = k_2 = 0$ was assumed (table 3). As a result, the total number of ODEs in iPBPK-R of EBT for healthy subjects is $n = 14$.

Analysis. Having expressed iPBPK-R's reduced PBPK model and all its dependencies on parameters and adjustment factors as instance of (8) enables us to analyze iPBPK-R's estimation capabilities and stability. We want to emphasize that iPBPK-R uses standard numerical solvers for ODE integration and optimization. The theoretical framework developed in section 3.5 is *not* used to compute the solutions but to analyze the solution quality and soundness of the approach.

We base the discussion below on analyzing the eigendecompositions of the upper and lower matrix approximations \mathbf{A}^+ and \mathbf{A}^- of the system operator matrix \mathbf{A} of (8). The element-wise distance $|a_{i,j}^+ - a_{i,j}^-|$ is small as required, and both \mathbf{A}^+ and \mathbf{A}^- are indeed simple matrices.

The first observation is that while the EBT iPBPK-R model has 14 compartments for the purpose of modeling mass balance, the underlying dynamical system has only 7 compartments. The 5 source/sink compartments and the 2 further helper compartments lead to a null space of dimension 6 and can be disregarded in the discussion. Inspection of Fig. 7 and the simulated curves in all 7 compartments (shown in [14]) as well as Fig. 9 indicate that at most four distinctive estimable modes θ_i of the eigendecomposition are present in the liver compartment. Thus, the $T = 11$ sampling points and the associated noise is sufficient to estimate the modes to a reasonable accuracy level. The measurements are clustered at the early transient phase and thus allow for estimating non-linear saturation due to Michaelis-Menten behavior.

Secondly, the number of adjustment parameters that can be distinguished is limited to $M = 7$ functionally independent α_i at max. iPBPK-R has $K = 9$ adjustment parameters, and thus they must have a functional (non-linear) dependence. The dependence is actually shown in [14] as the four main levers that shape the $^{14}\text{CO}_2$ production rate curve. The condition that the adjustment factor vector \vec{r} needs to be as close to $\mathbf{1}_M$ as possible disambiguates the functional dependency. This regularizes the estimates and pushes them towards the global optimum analogous to the arguments presented in [1]. Adding to estimation stability is the nested optimization procedure employed by iPBPK-R, presented next.

5 Parameter Estimation in iPBPK-R

Overview. Multiple-parameter estimation via iPBPK-R is an optimization problem (11) for a subset of parameters in the system of ODEs in eq. (3), collected in a K -dimensional parameter vector \vec{r} as defined in (18). This optimizes a subset of drug flow terms (see (19) and table 2) by minimizing the distance between observed and simulated data. Some of the optimized adjustment factors will provide parameter estimates for activities of metabolic enzyme and drug transporters in individuals, in non-renal drug clearance, providing an indirect measurement procedure for these parameters. We developed an EBT specific objective function (an instance of eq. (12)) consisting of a distance measure and penalty terms that regularizes the problem.

$^{14}\text{CO}_2$ measurement. Remember from section 3.4 that $B(t)$ denotes the $^{14}\text{CO}_2$ production rate at time t and is a function $\mathcal{F}(\cdot)$ of the solution vector $\vec{C}(t)$. Further, $\dot{C}_{i^*}(t)$ denotes the derivative of concentration in the i^* compartment. In our case this is the Liver compartment, which metabolizes the drug into $^{14}\text{CO}_2$. Thus,

$$B(t) = \mathcal{F}(\vec{C}(t)) = \dot{C}_{i^*}(t)$$

describes $^{14}\text{CO}_2$ production rate measured via breath and is an instance of (9).

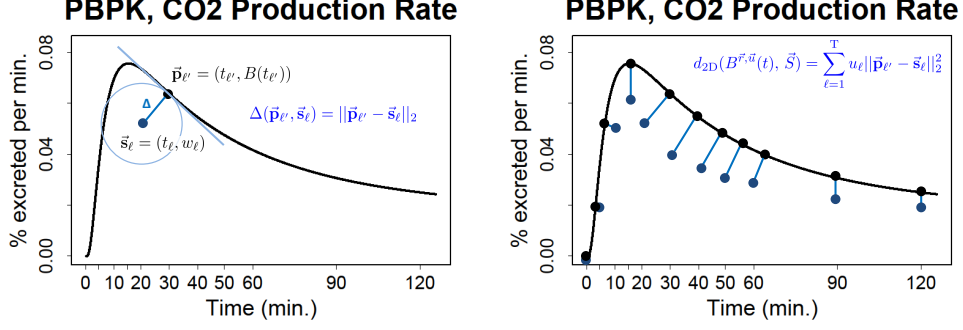


Figure 6: 2D L_2 norm and 2D distance measure.

Configuration. Next we define the constant configuration vector

$$\vec{u} = (h, \vec{h}', \vec{h}'', (u_\ell)_\ell, u_b, u_c, u_d, u_x)$$

with a scalar h , K -dimensional vectors \vec{h}' and \vec{h}'' , and weights u_ℓ . h is the indicator used in eq. (21) while \vec{h}' and \vec{h}'' configure penalties for adjustment factors in \vec{r} . $(u_\ell)_\ell$ is weighting the measurement while u_b , u_c , u_d , and u_x are penalty weights in eq. (13).

Distance measure. Clinical measurements may be slightly shifted relative to the planned time point. We introduce a 2D distance (Fig. 6) between simulated and measured $^{14}\text{CO}_2$ data points that allows some (penalized) misalignment in x direction in addition to mismatch in y direction.

We define the ℓ th measurement point measured at time t_ℓ as $\vec{s}_\ell = (t_\ell, w_\ell)$ and the point $p_{\ell'} = (t_{\ell'}, B(t_{\ell'}))$ where

$$t_{\ell'} = \arg \min_{t' \in [t_\ell - \delta, t_\ell + \delta]} \|(t', B(t')) - (t_\ell, w_\ell)\|_2$$

for an appropriately chosen δ . We collect the T measurements \vec{s}_ℓ at time points t_ℓ as vector $\vec{S} = ((t_\ell, \vec{s}_\ell))_\ell$. Then the 2D distance between the simulated function $B(t)$ parameterized by \vec{r} and \vec{u} and the measurement vector \vec{S} , is defined as

$$d_{2D}(B^{\vec{r}, \vec{u}}(t), \vec{S}) = \sum_{\ell=1}^T u_\ell \|\vec{p}_{\ell'} - \vec{s}_\ell\|_2^2. \quad (24)$$

Objective function in iPBPK-R. We now state the full objective function as used for EBT (an instance of (12)),

$$\Psi_{2D}^{\vec{r}, \vec{u}}(B^{\vec{r}, \vec{u}}(t), \vec{S}) = d_{2D}(B^{\vec{r}, \vec{u}}(t), \vec{S}) + \pi(\vec{r}, \vec{u}) \quad (25)$$

with the components of the penalty and regularization term $\pi(\vec{r}, \vec{u})$ defined in table 1, instantiating (13): eq. (28) avoids biologically unrealistic parameter estimation by penalizing distance from IVIVE values, eq. (29) ensures non-negative estimates, eq. (30) penalizes peak height deviation from the data peak, and eq. (31) penalizes mis-alignment in the x direction. Variants of $\Psi_{2D}^{\vec{r}, \vec{u}}(\cdot, \cdot)$ adjusted to problem settings can be configured via the configuration vector \vec{u} .

Parameter estimation. Biologically plausible multiple-parameter estimation via iPBPK-R for measured samples \vec{S} is done by solving the optimization problem

$$\vec{r} = \arg \min_{\vec{r}} \Psi_{2D}^{\vec{r}, \vec{u}}(\mathcal{F}, \vec{S}) \quad \text{for configuration } \vec{u} \quad (26)$$

to estimate the most likely parameter vector \vec{r} . The full optimization space for EBT allows for 7 independent parameters, but in practice not all of them are strongly influencing the fit. Depending on the goodness-of-fit of modeling, some less influential parameters in \vec{r} can be fixed as constants and not necessarily be optimized. This is achieved through appropriate setting of the indicator vectors \vec{h}' and \vec{h}'' .

Bias	$\nu(\vec{r}, \vec{h}') = \ \text{diag}(\vec{h}')(\vec{r} - \vec{r}_0)\ _2^2$ with $\vec{h}' \in \{0, 1\}^K$	(28)
Lower bound	$\rho(\vec{r}, \vec{h}'') = \sum_{i=1}^K h''_i \min(r_i - r_i^L, 0)^2$ with $\vec{h}'' \in \{0, 1\}^K$	(29)
Drift	$\epsilon(\vec{r}) = \left(\max_{t \in [t_0, t_T]} B^{\vec{r}, \vec{u}}(t) - \max_{\ell=1, \dots, T} w_\ell \right)^2$	(30)
X-shift	$\psi(\vec{r}) = \sum_{\ell=1}^T t_{\ell'} - t_\ell $	(31)

Table 1: Regularization penalty terms.

Combined pre/post treatment estimates. The focus of clinical pharmacology studies often is the impact of a treatment (in our case dialysis) on biological parameters. In a kidney disease study where EBT is used before and after the patients receive dialysis, our goal is to apply iPBPk-R to these two data series to estimate the effect of dialysis on biological parameters of individual patients. We assume that *independent parameters* remain unchanged while *co-optimization parameters* change from pre-dialysis to post-dialysis. To estimate both co-optimization parameters and independent parameters we developed a co-optimization method as discussed below.

The same data sampling procedure using configuration \vec{u} is performed pre and post dialysis, leading to data sets \vec{S}_1 and \vec{S}_2 . From the corresponding parameter estimates \vec{r}_1 and \vec{r}_2 we derive the simulated breath curves $B_1(t)$ and $B_2(t)$. The parameters vectors \vec{r}_1 and \vec{r}_2 are not independent: we set

$$\vec{r}_1 = \vec{r}_c \oplus \vec{r}_{i,1} \quad \text{and} \quad \vec{r}_2 = \vec{r}_c \oplus \vec{r}_{i,2}$$

where \vec{r}_c denotes the co-optimized parameters and $\vec{r}_{i,j}$ the independent parameters, and \oplus denotes the vector direct sum. With this setup we define the co-optimization problem as

$$(\vec{r}_1, \vec{r}_2) = \arg \min_{\vec{r}_c, \vec{r}_{i,1}, \vec{r}_{i,2}} \sum_{j=1}^2 \Psi_{2D}^{\vec{r}_c \oplus \vec{r}_{i,j}, \vec{u}}(B_j^{\vec{r}_c \oplus \vec{r}_{i,j}, \vec{u}}(t), \vec{S}_j). \quad (27)$$

Parameters beyond \vec{r} defined in (18) may need to be included in \vec{r}_1 and \vec{r}_2 , and \vec{u} needs to be chosen carefully to model pre/post dependencies and address particular research.

Numerical methods and implementation. We implemented the iPBPk-R in the R system. We used the R function `ode` in the `deSolve` package that implements a suite of ODE solvers, including explicit and implicit solvers, adaptive solvers, and Runge Kutta solvers [9] [53]. Optimization was performed using the `L-BFGS-B` and `BFGS` algorithms provided by the R function `optim` that implements quasi-Newton method with or without a limited-memory modification, respectively [8]. The nested optimization used for co-optimizing estimates is implemented via a generalized Hill Climbing approach. Optimization of the independent parameter vectors $\vec{r}_{i,1}$ and $\vec{r}_{i,2}$ were performed first independently in a inner loop. Optimization of the co-optimization parameter vector \vec{r}_c was implemented in an outer loop. This iteration was performed iteratively until sufficient convergence.

6 Examples and Results

This section provides a brief summary of two applications of iPBPk-R and discusses the results with respect to method feasibility and soundness. The detailed results and pharmacological interpretations of the first application had been described in [14]. In addition, the preliminary results of the second application was presented as a poster [15].

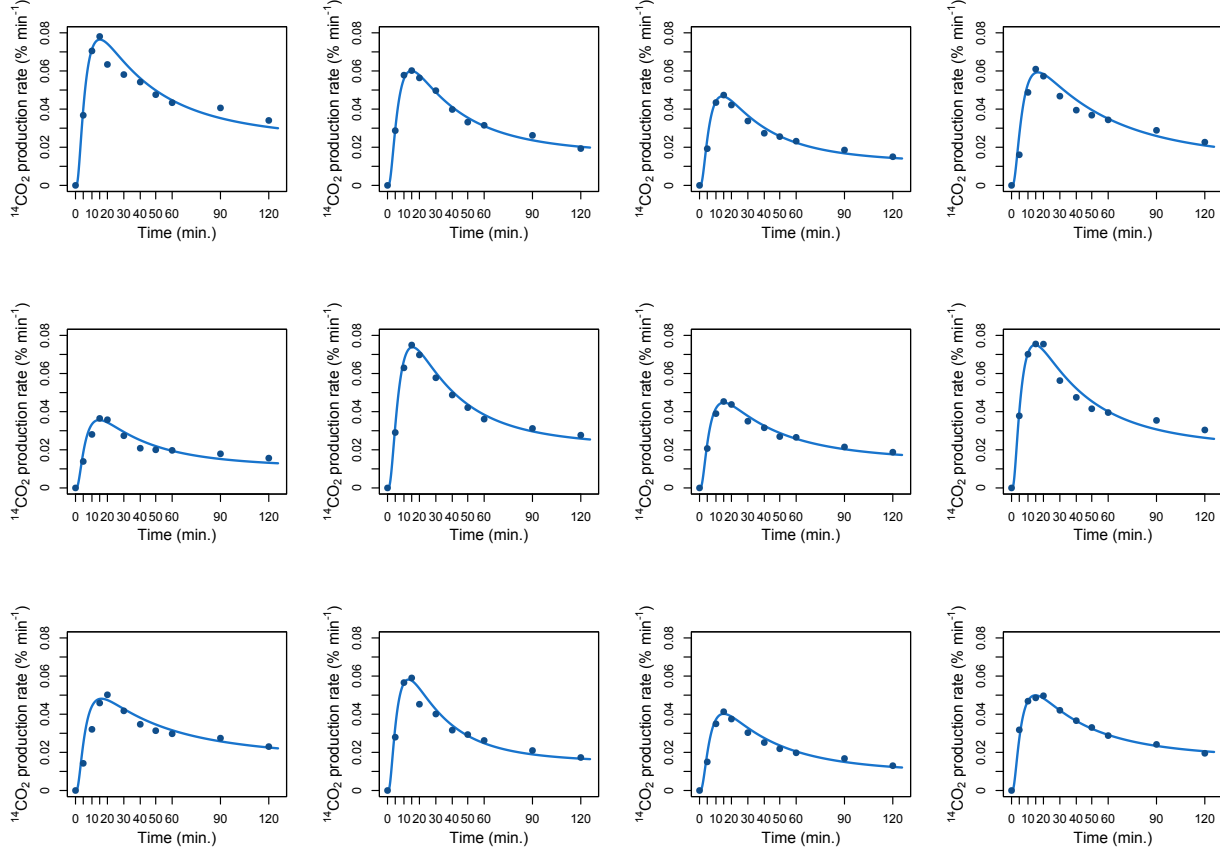


Figure 7: iPBPK-R model fit to the $^{14}\text{CO}_2$ production rate-time curves of 12 healthy subjects. Adapted from Franchetti et al. [14] with permission of ASPET.

6.1 Estimating Parameters in Healthy People

We model $^{14}\text{CO}_2$ production rate data obtained from 12 healthy subjects in an EBT study to estimate biological parameters. The study design is described in section 2.3 and [35]. Briefly, 12 healthy subjects received a single IV dose of ^{14}C -erythromycin (0.074 mmol), and breath samples were collected immediately at 11 time points within two hours including the baseline time point of EBT. $^{14}\text{CO}_2$ production rates in the collected breath samples were calculated.

The iPBPK-R model structure and parameters of the system of ODEs were shown Fig. 4, Fig. 5, and table 4. The initial values of the input parameters are shown in table 3, including IVIVE values can be found in [14]. Through an initial manual investigation we first identified that nine parameters were either impacting the shape of the simulated rate-time curve $B(t)$ or biologically relevant parameters (see table 4)

$$J_a, J_b, J_c, Q_{\text{cyp}}, V_7, P_3, \mu_3, Q_3, \text{ and } Q_{67},$$

and their respective adjustment factors to be optimized,

$$\beta_6, \beta_{7,1}, \beta_{7,2}, \alpha_7, \zeta_7, \gamma_3, \alpha_3, \kappa_{35}, \text{ and } \kappa_{67}.$$

The results are summarized in Fig. 7. The iPBPK-R model fit well for individual $^{14}\text{CO}_2$ production rate-time curves as result of parameter optimization. Sensitivity analysis and analysis following section 3.5 established that the parameter estimates are sound. Among the optimized adjustment factors $\beta_6, \beta_{7,1}, \beta_{7,2}, \alpha_7, \zeta_7,$ and κ_{67} were associated with the Liver compartment, where activities in non-renal elimination pathways were target of the published research. The parameter estimates are shown in Fig. 8. While $\beta_{7,1}$

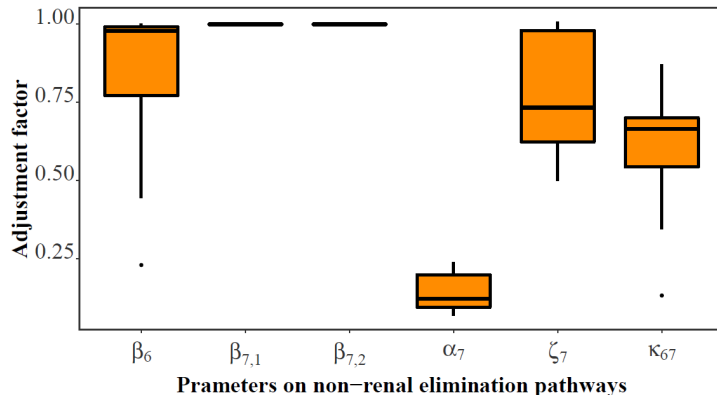


Figure 8: Box plot of estimated adjustment factors in 12 subjects. Adapted from [14] with permission of ASPET.

and $\beta_{7,2}$ did not have impact on the model fit in the figure, we forced them into the iPBPK-R model for mechanistic considerations.

In exploring the simulation results, the estimated α_7 were stratified by gender. Analysis led to the finding of gender difference in enzyme activity of the liver as reported in [14]. This aligned with literature describing a gender difference in expression of the same enzyme in human liver samples [60], a fact not actively modeled in iPBPK-R. While this finding is well beyond the scope of method evaluation, similar evidence will help us to build confidence in steps towards clinical utility. Production simulation runs required about 10 CPU hours per subject on the *Bridges* supercomputer at PSC.

6.2 Co-Estimation Pre- and Post Dialysis

The second example is the application of iPBPK-R to the $^{14}\text{CO}_2$ production rate data obtained from 12 patients with kidney disease in an EBT study. The study design of the EBT study is described in [34] and [15]. Briefly, 12 patients received a single IV dose of ^{14}C -erythromycin before taking a 4-hour dialysis. Two hours post-dialysis these patients received another single IV dose. In each EBT breath samples were collected immediately at 11 time points within two hours of IV, including the baseline time point of EBT. Subsequently $^{14}\text{CO}_2$ production rates were calculated for the pre- and post-dialysis EBTs. The model structure and the system of ODEs were similar to those in the first example, and it was assumed that the reduced activity of mass flow is non-competitive. The mass flow from Kidney to Urine (see Fig. 4) was removed assuming no kidney function in patients and drug removal by dialysis was assumed negligible. Further, a pre/post carry-over effect was added that carried the trailing drug concentration from the pre-EBT into the post-EBT.

The same optimization parameters were selected as in the first example. Optimization was implemented via nested co-optimization and the adjustment factor α_7 was optimized in the inner loop to independently estimate the adjustment factors pre- and post-dialysis for linear CYP3A4 activity. Inhibition parameters associated with drug transporters were also estimated independently so that the change in the nonlinear activity of each drug transporter could be evaluated by comparing the inhibition parameters pre- and post-dialysis.

We show the resulting iPBPK-R model fit for two patients in Fig. 9. The iPBPK-R model fit the individual $^{14}\text{CO}_2$ production rate-time curves pre- and post-dialysis well. Again, sensitivity analysis and analysis following section 3.5 establishes that the parameter estimates are sound. In further analysis shown in [15], activities of CYP3A4 and drug transporter activities were compared across dialysis in each patient so that the effect of dialysis on the non-renal elimination pathways could be evaluated. A production simulation run required 24 CPU hours per patient.

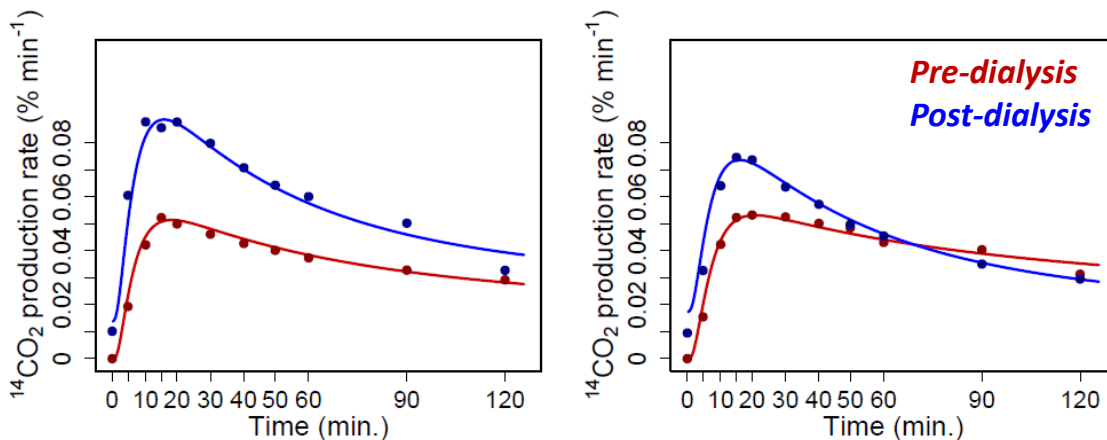


Figure 9: iPBPK-R model fit to the $^{14}\text{CO}_2$ production rate-time curves of two patients with dialysis.

7 Discussion

7.1 iPBPK-R Summary

Pharmaceutical application. *iPBPK-R* allows us to estimate multiple physiological parameters in individuals using a single dose of a single probe drug. This mechanistic indirect measurement approach allows for *in vivo* activities (e.g., of CYP3A4 and drug transporters) to be *estimated for a particular individual*. Activities can be estimated pre/post intervention or disease progression for longitudinal monitoring. With iPBPK-R mechanistic sources of inter-individual variability can be identified, and we anticipate it to be eventually useful to enable personalized dosing of narrow therapeutic drugs based on the estimated physiological activity.

The focus of this paper is to establish iPBPK-R as a method and analyze its properties and performance guarantees for future uses in emerging breath biopsy/biomarker research [7, 19]. To establish iPBPK-R as an clinically aiding tool, well-designed large-scale clinical trials need to be conducted in a step-wise manner in a probe development context. Such an undertaking will require resources beyond our small group, but will be aided by the foundations laid by this paper. Potential future fields of application include oncology, pediatrics, nephrology, and severe health conditions.

Key insight. Our approach uses *production rate* data modeled as the first derivative of drug concentration data in model fitting. Through the dynamic changes in the early (transient) phase of the production rate-time curve, parameters of both rate-limiting and non-rate-limiting steps can be estimated. As the probe dose is low, detailed sampling of the initial phase of drug concentration can reveal the characteristics of the system, similar to how impulse responses are used to characterize systems of interest in signal processing [37]. In future work we will investigate ODE-imposed coupling of multiple drug concentration datasets per individual.

Model and estimation. We used a reduced order model (that still qualifies as full PBPK model [48]) in iPBPK-R where the number of compartments was limited so that model parameters can be estimable. Reducing the number of parameters is essential since the main purpose of this method is not to predict PK profiles for populations but to back estimate multiple physiological parameters of a nonlinear system of ODEs in particular individuals. We paid particular attention at how to regularize the optimization problem to enable convergence without skewing the estimation results.

Use of biological knowledge as reference. A priori knowledge obtained from literature (e.g., *IVIVE*) was used as reference values in parameter optimization to aid convergence to biologically plausible estimates. While a global minimum in parameter optimization is not guaranteed, we find good biologically plausible estimates. Our nested co-optimization approach allows us to partition parameters into independent and common parameters when using combined pre/post intervention data sets. This allows us to identify changes in physiological activities per person and thus differentiate the individuals based on the physiological activities that cannot be measured directly.

Computational cost and time. iPBPk-R was implemented using R leading to high computational cost (150,000 CPU hours total over the course of its development) and long run times (days per optimization run), utilizing the *Bridges* supercomputer at the Pittsburgh Supercomputing Center (PSC). Efficiency could be gained by switching to C++ at the cost of substantial development effort.

7.2 Comparison to Other Approaches

Classical prediction vs. estimation. A *cocktail approach* where a subject takes multiple activity-specific probe drugs is the standard method to indirectly estimate different biological activities [52] [62]. The group-wide activities associated with the respective drugs are statistically estimated, in contrast to individual estimates in iPBPk-R.

Conventional *population PBPK modeling* is statistics-based modeling for an entire population. It uses a limitless number of parameters to capture all foreseen variabilities in various clinical scenarios and IVIVE values are used as fixed input for simulations and prediction. In population PBPK modeling researchers can assume some distributions on the property parameters and generate distributional parameter inputs using Monte Carlo approaches or similar methods. As a result the simulated drug concentration-time curves will vary broadly and have to be statistically summarized (median, 95% CI, etc.).

Due to the broader range of simulation curve outputs and the large number of input parameters, PBPK modeling is usually used to construct the statistical bounds of drug safety and/or efficacy. In contrast, iPBPk-R was developed for estimating multiple physiological parameters of individuals. It enables multiple parameter estimation with a single probe via individual model fit.

Mechanistic vs. statistical modeling. iPBPk-R does not use distributional assumptions for parameters but uses them as reference values in the optimization procedure to estimate individual parameters. Using a statistical population PBPK model would likely produce biased estimates since many co-dependent physiological parameters are treated as independent in their distributional assumptions. IVIVE values are not necessarily clinically relevant population means, as they extrapolate *in vitro* experimental values based on simple mathematical models. In contrast we estimate per-individual deviations from IVIVE values to overcome their limitation.

Validation and model selection. In population PBPK modeling, a model validation step is required to confirm a model’s predictive ability when observed data become available. In contrast, iPBPk-R uses a pre-determined model that is fit to individual observed data to estimate parameters given the model structure. This approach is inherently different from model validation for prediction: the model either works as is evident from good fit and biologically plausible parameter estimates, or a better PBPK model needs to be developed re-opening the PK modeling process.

With respect to model fitting, there is no formal statistical test to compare two sets of ODE parameters that have functional dependencies within each set. However, it is generally understood that such two sets of parameters for the same nonlinear system of ODEs result in quite different sets of solutions that will have obvious differences in model fit. The theory and result presented shows that our application examples were free from overfitting and estimation issues. Our approach is not compatible with covariate selection in general PK modeling (e.g., nonlinear mixed models) where a covariate term is linealized and covariates are added or dropped based on some statistical threshold.

PBPK software. A number of software tools are available to conduct PBPK simulations. The Simcyp Simulator by Certara USA, Inc. [22] provides PBPK modeling for a virtual populations of interest. NONMEM by ICON [39] is FORTRAN-based biomathematical modeling software that allows users to explicitly specify mathematical models [45]. ADAPT 5 is another FORTRAN-based software [36] [3]. These systems require programming in legacy languages like FORTRAN in combination with system-specific commands and features, which hampers more customized PBPK modeling and method research. Thus, iPBPk-R was developed using the free statistics-centered R system [10]. Powerful optimization is available for model fitting, and parameter estimation across a wide range of observed data types (including breath rate data) can be implemented, as can parameter co-optimized across clinical intervention we use to correlate behavior before and after dialysis for kidney disease patients.

8 Conclusions

We presented iPBPk-R, a novel signal processing based *indirect measurement* method, which is useful to simultaneously estimate multiple physiological parameters in individuals using clinical observed data. For this purpose, breath biopsy data is particularly well-suited as it can be modeled as the first derivative of drug concentration data and sampled at high clinical frequency to resolve early transients of drug behavior. The core of iPBPk-R is the joint estimation of multiple biological parameters via fitting of a nonlinear system of ODEs across all measurement data of an individual. We establish the mathematical foundations and computational framework of the parameter estimation and provide evidence that the parameter estimates obtained by iPBPk-R are stable and accurate.

We analyze the method's feasibility and establish its soundness, building on two published applications of iPBPk-R. Excellent model fits were achieved in individuals where multiple dependent parameters are estimated, and biological findings derived from iPBPk-R were compatible with independent biological experiments. Based on this early success with EBT we anticipate a path to eventual utilization of iPBPk-R in large-scale clinical trials, which may aid steps towards probe and biomarker development in personalized medicine. In future work other types of clinical datasets beyond EBT including multiple coupled drug concentration datasets per individual will be used.

Appendix: Tables

Drug mass flows
$q_{8;\dot{2}} = M/t_0$ for $0 \leq t \leq t_0$, and 0 else
$q_{2;\dot{1}} = Q_1(C_2 - \frac{C_1}{P_1})$, $q_{1;\dot{5}} = Q_1(\frac{C_1}{P_1} - C_5)$, $q_{4;\dot{2}} = Q_4(\frac{C_4}{P_4} - C_2)$
$q_{4;\dot{10}} = \delta G_{fr} \frac{f_b}{P_4} C_4 + MM_{\eta, J_b, K_b}(\frac{f_b}{P_4} C_4)$, $q_{7;\dot{11}} = Q_{cyp} \frac{f_7}{P_{7p}} C_7$
$q_{5;\dot{4}} = Q_4(C_5 - \frac{C_4}{P_4})$, $q_{3;\dot{2}} = Q_3(\frac{C_3}{P_3} - C_2)$, $q_{5;\dot{3}} = Q_3(C_5 - \frac{C_3}{P_3})$
$q_{3;\dot{9}} = \mu_3 C_3$, $q_{5;\dot{6}} = Q_5 C_5$, $q_{6;\dot{2}} = Q_2 C_{2 6}$
$q_{6;\dot{7}} = MM_{J_a, K_a}(\frac{f_6}{P_{6p}} C_6) + Q_{67}(\frac{f_6}{P_{6p}} C_6 - \frac{f_7}{P_{7p}} C_7)$
$q_{7;\dot{12}} = MM_{J_b, K_b}(\frac{f_7}{P_{7p}} C_7) + MM_{J_c, K_c}(\frac{f_7}{P_{7p}} C_7)$

Table 2: Mass flows of ^{14}C -erythromycin in Fig. 4.

Parameter	definition
Q_1, Q_{67}	total blood flow and passive diffusion Comp. 6 and 7
Q_2, Q_5	blood flow Compartment 6 to 2 and Compartment 5 to 6
Q_3, Q_4	blood flow in and out of Compartment 3 and 4
P_i, P_{ip}	partition coefficient of Compartment i to blood and plasma
f_i, f_{ib}	fraction unbound in Compartment i and blood
δG_{fr}	estimated GFR, scaled with GFR filtration fraction δ
J_a, J_b, J_c	maximum velocity of drug transporter a, b, and c
K_a, K_b, K_c	Michaelis-Menten constant of drug transporter a, b, and c
η	distribution ratio of transporter b in Compartment 4 to 7
μ	exponential decay parameter of the parent drug
Q_{cyp}	CYP3A4 clearance (calculated IVIVE value)
k_1	distribution rate of $\text{H}^{14}\text{CO}_3^-$ from liver to pool (0.0 [55])
k_2	distribution rate of $\text{H}^{14}\text{CO}_3^-$ from pool to liver (0.0 [55])
k_3	excretion rate constant of $^{14}\text{CO}_2$ in the liver cell
ϕ	conversion of $^{14}\text{CO}_2$ from mol to Ci (here, $\phi = 1$)

Table 3: Drug flows parameters of ^{14}C -erythromycin.

Adj. factor	Definition: <i>adjustment factor of</i>
α_3	exponential decay in Other Organs compartment
α_7	CYP3A4 activity in Liver Cell compartment
β_6	drug transporter a in the liver
$\beta_{7,1}$	drug transporter b in the liver
$\beta_{7,2}$	drug transporter c in the liver
γ_3	partition coefficient of Other Organs to blood
ζ_7	volume of Liver Cell compartment
κ_{35}	arterial blood flow into Other Organs compartment
κ_{67}	passive diffusion between ES and Liver Cell comp.

Table 4: Adjustment factors in iPBPK-R for EBT.

Entries of \mathbf{X} , $\tilde{\mathbf{Y}}$ and \mathbf{D}
$x_{1,1} = -2\frac{Q_1}{V_1P_1}, x_{1,2} = \frac{Q_1}{V_1}, x_{1,5} = \frac{Q_1}{V_1}, x_{2,1} = \frac{Q_1}{V_2P_1},$
$x_{2,2} = -\frac{Q_1+Q_3+Q_4}{V_2}, x_{2,3} = \frac{Q_3}{\gamma_3V_2P_3},$
$x_{2,4} = \frac{Q_4}{V_4P_4}, x_{2,6} = \frac{Q_2}{V_2P_6}$
$x_{3,2} = \frac{Q_3}{V_3}, x_{3,3} = -\frac{(\kappa_{35}+1)\frac{Q_3}{\gamma_3P_3} + \alpha_3\mu_3}{V_3},$
$x_{3,5} = \frac{\kappa_{35}Q_3}{V_3},$
$x_{4,2} = \frac{Q_4}{V_4}, x_{4,4} = -\frac{2Q_4+\delta G_{fr}f_b}{V_4P_4}, x_{4,5} = \frac{Q_4}{V_4},$
$x_{5,1} = \frac{Q_1}{V_5P_1}, x_{5,3} = \frac{\kappa_{35}Q_3}{\gamma_3V_5P_3}, x_{5,4} = \frac{Q_4}{V_5P_4},$
$x_{5,5} = -\frac{Q_1+\kappa_{35}Q_3+Q_4}{V_5}, x_{5,6} = -\frac{Q_5}{V_5},$
$x_{6,5} = \frac{Q_5}{V_6}, x_{6,6} = -\frac{1}{V_6} \left(\frac{\kappa_{67}Q_{67}f_6}{P_{6p}} + \frac{Q_2}{P_6} \right), x_{6,7} = \frac{\kappa_{67}Q_{67}f_6}{V_6P_{7p}},$
$x_{7,6} = \frac{\kappa_{67}Q_{67}f_6}{\zeta_7V_7P_{6p}}, x_{7,7} = -\frac{(\kappa_{67}Q_{67}+\alpha_7Q_{cyp})f_7}{\zeta_7V_7P_{7p}}, x_{9,3} = \frac{\alpha_3\mu_3}{V_3},$
$x_{10,4} = \frac{\delta G_{fr}f_b}{V_4P_4}, x_{11,7} = \frac{\alpha_7Q_{cyp}f_7}{\zeta_7V_7P_{7p}},$
$x_{13,7} = \frac{\alpha_7Q_{cyp}f_7}{\zeta_7V_7P_{7p}}, x_{13,13} = -k_3, x_{14,13} = \phi k_3$
$y_{4,4} = -MM_{\beta_{7,1}\eta J_b, K_b}$
$y_{6,6} = -MM_{\beta_6 J_a, K_a}$
$y_{7,6} = MM_{\beta_6 J_a, K_a}$
$y_{7,7} = -(MM_{\beta_{7,1} J_b, K_b} + MM_{\beta_{7,2} J_c, K_c})$
$y_{10,4} = MM_{\beta_{7,1}\eta J_b, K_b}$
$y_{12,7} = MM_{\beta_{7,1} J_b, K_b} + MM_{\beta_{7,2} J_c, K_c}$
$d_4 = \frac{f_b}{V_4P_4}, d_6 = \frac{f_6}{V_6P_{6p}}, d_7 = \frac{f_7}{\zeta_7V_7P_{7p}}$

Table 5: Entries of matrices \mathbf{X} , $\tilde{\mathbf{Y}}$, and \mathbf{D} .

References

- [1] Navid Azizan and Babak Hassibi. Stochastic gradient/mirror descent: Minimax optimality and implicit regularization. *arXiv preprint arXiv:1806.00952*, 2018.
- [2] Z. E. Barter, M. K. Bayliss, P. H. Beaune, A. R. Boobis, D. J. Carlile, R. J. Edwards, J. B. Houston, B. G. Lake, J. C. Lipscomb, O. R. Pelkonen, G. T. Tucker, and A. Rostami-Hodjegan. Scaling factors for the extrapolation of in vivo metabolic drug clearance from in vitro data: reaching a consensus on values of human microsomal protein and hepatocellularity per gram of liver. *Curr Drug Metab*, 8(1):33–45, 2007.
- [3] USC BMSR. Adapt 5 user’s guide. 2019.
- [4] Hans Georg Bock. *Numerical treatment of inverse problems in chemical reaction kinetics*, pages 102–125. Springer, 1981.
- [5] M. Chiba, Y. Ishii, and Y. Sugiyama. Prediction of hepatic clearance in human from in vitro data for successful drug development. *AAPS J*, 11(2):262–76, 2009.
- [6] Paulo Cortez. *Modern optimization with R*. Springer, 2014.
- [7] Sagnik Das and Mrinal Pal. Non-invasive monitoring of human health by exhaled breath analysis: A comprehensive review. *Journal of The Electrochemical Society*, 167(3):037562, 2020.
- [8] The R foundation. optim. 2019.
- [9] The R foundation. Package ‘desolve’. 2019.
- [10] The R foundation. What is r? introduction to r. 2019.
- [11] Franz Franchetti, Tze Meng Low, Doru Thom Popovici, Richard M Veras, Daniele G Spampinato, Jeremy R Johnson, Markus Püschel, James C Hoe, and José MF Moura. Spiral: Extreme performance portability, special issue on ”from high level specication to high performance code”. *Proceedings of the IEEE*, 106(11):1935–1968, 2018.
- [12] Franz Franchetti, de Frédéric Mesmay, Daniel McFarlin, and Markus Püschel. *Operator language: A program generation framework for fast kernels, in IFIP Working Conference on Domain Specific Languages (DSL WC)*, volume 5658, pages 385–410. Springer, 2009.
- [13] Y. Franchetti. *Individualized Physiologically Based Pharmacokinetic Modeling of Rate Data (iPBPK-R): A Novel Approach to Estimate the Effect of Kidney Disease on Nonrenal Elimination Pathways [dissertation]*. University of Pittsburgh School of Pharmacy, Pittsburgh, PA, 2020.
- [14] Y. Franchetti and T. D. Nolin. Simultaneous assessment of hepatic transport and metabolism pathways with a single probe using individualized pbpk modeling of (14)co2 production rate data. *J Pharmacol Exp Ther*, 371(1):151–161, 2019.
- [15] Yoko Franchetti and Thomas D Nolin. Application of individualized physiologically-based pharmacokinetic modeling of rate data (ipbpk-r) to estimate the effect of hemodialysis on nonrenal clearance pathways. American Society of Nephrology.
- [16] RM Franke, CS Lancaster, CJ Peer, AA Gibson, AM Kosloske, SJ Orwick, RH Mathijssen, WD Figg, SD Baker, and Alex Sparreboom. Effect of abcc2 (mrp2) transport function on erythromycin metabolism. *Clin Pharmacol Ther*, 89(5):693–701, 2011.
- [17] LA Frassetto, S Poon, C Tsurounis, C Valera, and LZ Benet. Effects of uptake and efflux transporter inhibition on erythromycin breath test results. *Clin Pharmacol Ther*, 81(6):828–832, 2007.
- [18] Mendel Fygenon. Modeling and predicting extrapolated probabilities with outlooks. *Statistica Sinica*, pages 9–40, 2008.

- [19] E. Gaude, M. K. Nakhleh, S. Patassini, J. Boschmans, M. Allsworth, B. Boyle, and M. P. van der Schee. Targeted breath analysis: exogenous volatile organic compounds (evoc) as metabolic pathway-specific probes. *J Breath Res*, 13(3):032001, 2019.
- [20] Vivian Hutson, J Pym, and M Cloud. *Applications of functional analysis and operator theory*. Elsevier, 2 edition, 2005.
- [21] Vivian Hutson, J Pym, and M Cloud. *Introduction to nonlinear operators*, volume 200, book section 4, pages 115–146. Elsevier, 2005.
- [22] Certara USA Inc. Simcyp simulator: The standard for population-based pharmacokinetic modeling and simulation. 2019.
- [23] M. Jamei, F. Bajot, S. Neuhoff, Z. Barter, J. Yang, A. Rostami-Hodjegan, and K. Rowland-Yeo. A mechanistic framework for in vitro-in vivo extrapolation of liver membrane transporters: prediction of drug-drug interaction between rosuvastatin and cyclosporine. *Clin Pharmacokinet*, 53(1):73–87, 2014.
- [24] Dominic Jordan, Peter Smith, and Peter Smith. *Nonlinear ordinary differential equations: an introduction for scientists and engineers*, volume 10. Oxford University Press on Demand, 2007.
- [25] Tosio Kato. *Perturbation theory for linear operators*, volume 132. Springer Science & Business Media, 2013.
- [26] M. E. Krecic-Shepard, C. R. Barnas, J. Slimko, J. C. Gorski, I. W. Wainer, and J. B. Schwartz. In vivo comparison of putative probes of cyp3a4/5 activity: erythromycin, dextromethorphan, and verapamil. *Clin Pharmacol Ther*, 66(1):40–50, 1999.
- [27] E Kreyszig, H Kreyszig, and EJ Norminton. *H. and Norminton, EJ (2011) Advanced Engineering Mathematics*. Wiley, NY, Hoboken, NJ, 10 edition, 2011.
- [28] Y. Krivoruk, M. T. Kinirons, A. J. Wood, and M. Wood. Metabolism of cytochrome p4503a substrates in vivo administered by the same route: lack of correlation between alfentanil clearance and erythromycin breath test. *Clin Pharmacol Ther*, 56(6 Pt 1):608–14, 1994.
- [29] D. Kurnik, A. J. Wood, and G. R. Wilkinson. The erythromycin breath test reflects p-glycoprotein function independently of cytochrome p450 3a activity. *Clin Pharmacol Ther*, 80(3):228–34, 2006.
- [30] Kenneth Levenberg. A method for the solution of certain non-linear problems in least squares. *Quarterly of applied mathematics*, 2(2):164–168, 1944.
- [31] Donald W Marquardt. An algorithm for least-squares estimation of nonlinear parameters. *Journal of the society for Industrial and Applied Mathematics*, 11(2):431–441, 1963.
- [32] N. Marsousi, J. A. Desmeules, S. Rudaz, and Y. Daali. Usefulness of pbpk modeling in incorporation of clinical conditions in personalized medicine. *J Pharm Sci*, 106(9):2380–2391, 2017.
- [33] Thorsten G Müller and Jens Timmer. Fitting parameters in partial differential equations from partially observed noisy data. *Physica D: Nonlinear Phenomena*, 171(1-2):1–7, 2002.
- [34] Thomas D Nolin, Kofi Appiah, Scott A Kendrick, Phuong Le, Ellen McMonagle, and Jonathan Himmel-farb. Hemodialysis acutely improves hepatic cyp3a4 metabolic activity. *J Am Soc Nephrol*, 17(9):2363–2367, 2006.
- [35] Thomas D Nolin, Kofi Appiah, Scott A Kendrick, Ellen Phuong Le McMonagle, and Jonathan Him-melfarb. Effect of hemodialysis on hepatic cyp3a4 activity. *Clin Pharmacol Ther*, 79(2):23, PI–60, 2006.
- [36] Universtiy of Sourthern California Biomedical Simulation Resourse (USC BMSR). Adapt. 2019.
- [37] Alan V. Oppenheim and Ronald W. Schafer. *Discrete-Time Signal Processing*. Prentice Hall Press, 2009.

- [38] M Peifer and J Timmer. Parameter estimation in ordinary differential equations for biochemical processes using the method of multiple shooting. *IET Systems Biology*, 1(2):78–88, 2007.
- [39] ICON plc. Nonmem®: The gold standard software in population pharmacokinetic and pharmacokinetic-pharmacodynamic modelling. 2019.
- [40] N. J. Proctor, G. T. Tucker, and A. Rostami-Hodjegan. Predicting drug clearance from recombinantly expressed cyps: intersystem extrapolation factors. *Xenobiotica*, 34(2):151–78, 2004.
- [41] O Richter, P Nörtersheuser, and W Pestemer. Non-linear parameter estimation in pesticide degradation. *Science of the total environment*, 123:435–450, 1992.
- [42] L. P. Rivory and P. B. Watkins. Erythromycin breath test. *Clin Pharmacol Ther*, 70(4):395–9, 2001.
- [43] Laurent P Rivory, Kellie A Slaviero, Janelle M Hoskins, and Stephen J Clarke. The erythromycin breath test for the prediction of drug clearance. *Clinical pharmacokinetics*, 40(3):151–158, 2001.
- [44] A. Rostami-Hodjegan and G. T. Tucker. Simulation and prediction of in vivo drug metabolism in human populations from in vitro data. *Nat Rev Drug Discov*, 6(2):140–8, 2007.
- [45] Malcolm Rowland, Carl Peck, and Geoffrey Tucker. Physiologically-based pharmacokinetics in drug development and regulatory science. *Annual review of pharmacology and toxicology*, 51:45–73, 2011.
- [46] Malcolm Rowland and Thomas N Tozer. *Clinical pharmacokinetics and pharmacodynamics: Concepts and Applications*. Lippincott Williams and Wilkins Philadelphia, 4 edition, 2011.
- [47] Karen Rowland Yeo, Mohsen Aarabi, Masoud Jamei, and Amin Rostami-Hodjegan. Modeling and predicting drug pharmacokinetics in patients with renal impairment. *Expert review of clinical pharmacology*, 4(2):261–274, 2011.
- [48] J. E. Sager, J. Yu, I. Ragueneau-Majlessi, and N. Isoherranen. Physiologically based pharmacokinetic (pbpk) modeling and simulation approaches: A systematic review of published models, applications, and model verification. *Drug Metab Dispos*, 43(11):1823–37, 2015.
- [49] K Schittkowski. Parameter estimation in systems of nonlinear equations. *Numerische Mathematik*, 68(1):129–142, 1994.
- [50] Klaus Schittkowski. *Numerical data fitting in dynamical systems: a practical introduction with applications and software*, volume 77. Springer Science & Business Media, Boston, MA, 2002.
- [51] M. R. Shiran, N. J. Proctor, E. M. Howgate, K. Rowland-Yeo, G. T. Tucker, and A. Rostami-Hodjegan. Prediction of metabolic drug clearance in humans: in vitro-in vivo extrapolation vs allometric scaling. *Xenobiotica*, 36(7):567–80, 2006.
- [52] N. F. Smith, F. I. Raynaud, and P. Workman. The application of cassette dosing for pharmacokinetic screening in small-molecule cancer drug discovery. *Mol Cancer Ther*, 6(2):428–40, 2007.
- [53] Karline Soetaert, Thomas Petzoldt, and R. Woodrow Setzer. Package desolve: Solving initial value differential equations in r. Report, 2010.
- [54] J Stoer and R Bulirsch. Introduction to numerical analysis, 2. aufl., ser. *Texts in Applied Mathematics*, 12, 2013.
- [55] E. Sugiyama, A. Kikuchi, M. Inada, and H. Sato. The use of ¹³c-erythromycin as an in vivo probe to evaluate cyp3a-mediated drug interactions in rats. *J Pharm Sci*, 100(9):3995–4005, 2011.
- [56] Torsten Teorell. Kinetics of distribution of substances administered to the body, i: the extravascular modes of administration. *Archives internationales de pharmacodynamie et de therapie*, 57:205–225, 1937.

- [57] John Towns, Timothy Cockerill, Maytal Dahan, Ian Foster, Kelly Gaither, Andrew Grimshaw, Victor Hazlewood, Scott Lathrop, Dave Lifka, and Gregory D. Peterson. Xsede: accelerating scientific discovery. *Comput Sci Eng*, 16(5):62–74, 2014.
- [58] G. T. Tucker, J. B. Houston, and S. M. Huang. Optimizing drug development: strategies to assess drug metabolism/transporter interaction potential-toward a consensus. *Clin Pharmacol Ther*, 70(2):103–14, 2001.
- [59] P. B. Watkins. Noninvasive tests of cyp3a enzymes. *Pharmacogenetics*, 4(4):171–84, 1994.
- [60] R. Wolbold, K. Klein, O. Burk, A. K. Nussler, P. Neuhaus, M. Eichelbaum, M. Schwab, and U. M. Zanger. Sex is a major determinant of cyp3a4 expression in human liver. *Hepatology*, 38(4):978–88, 2003.
- [61] Ya-Xiang Yuan. Recent advances in numerical methods for nonlinear equations and nonlinear least squares. *Numerical algebra, control and optimization*, 1(1):15–34, 2011.
- [62] H. Zhou, Z. Tong, and J. F. McLeod. ”cocktail” approaches and strategies in drug development: valuable tool or flawed science? *J Clin Pharmacol*, 44(2):120–34, 2004.